Supporting Information

Macroscale and durable near-zero wear performance on steel surface achieved by natural ternary deep eutectic solvents

Qiulong Gao[ab], Shuwen Liu[ad], Yan Huang[ab], Kaiming Hou[ad], Zhangpeng Li[abcd*], Jinqing Wang[ab*], Shengrong Yang[ab]

[a] *State Key Laboratory of Solid Lubrication, Lanzhou Institute of Chemical Physics, Chinese Academy of Sciences, Lanzhou 730000, China.*

[b] *Center of Materials Science and Optoelectronics Engineering, University of Chinese Academy of Sciences, Beijing 100049, China.*

[c] *Yantai Zhongke Research Institute of Advanced Materials and Green Chemical Engineering, Yantai 264006, China.*

[d] *Qingdao Center of Resource Chemistry & New Materials, Qingdao 266000, China.*

[*] Corresponding authors: zhangpengli@licp.cas.cn (Z. Li); jqwang@licp.cas.cn (J. Wang)

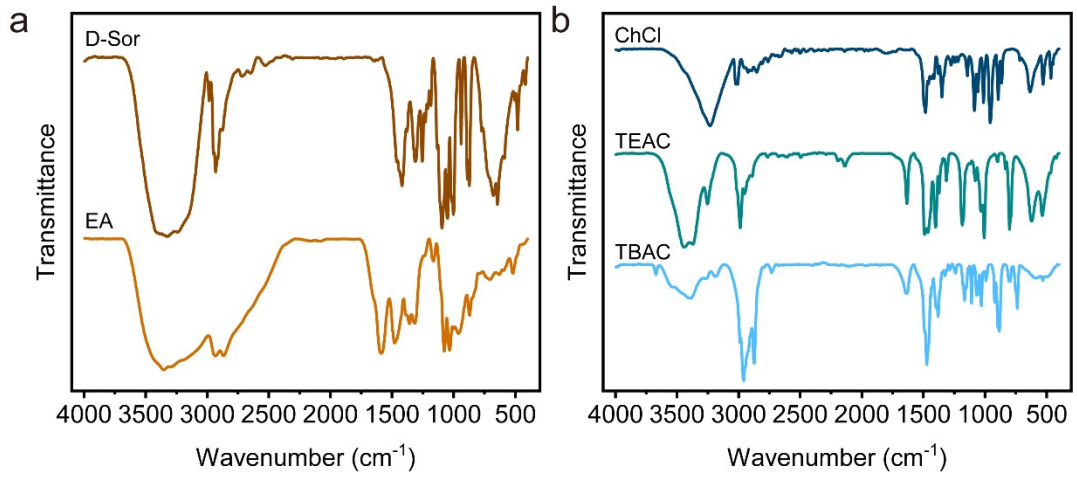

Fig. S1 FTIR spectra of (a) D-Sor and EA and (b) ChCl, TEAC and TBAC.

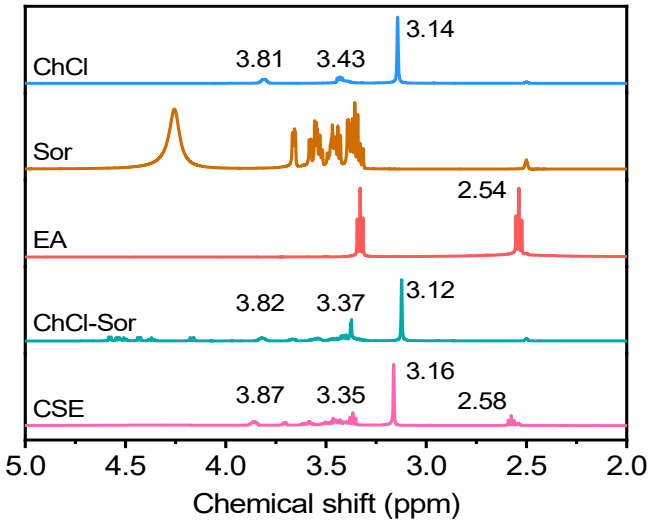

Fig. S2 ^{1}H NMR spectra of ChCl, Sor, EA, ChCl-Sor and CSE TDES.

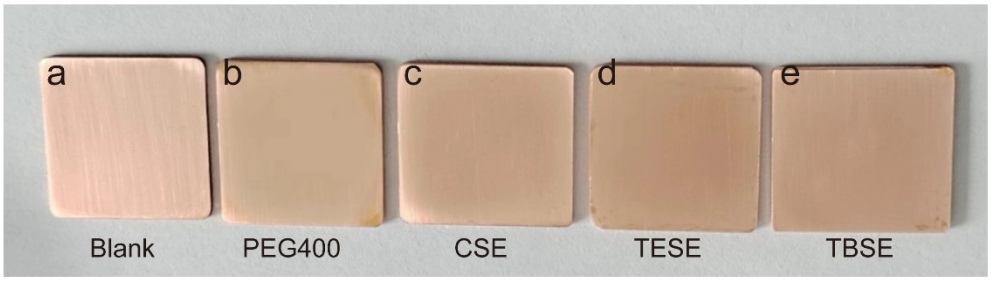

Fig. S3 Copper strips images exposed to PEG400 oil and the as-synthesized TDESs. (a) Blank, (b) PEG400, (c) CSE, (d) TESE and (e) TBSE.

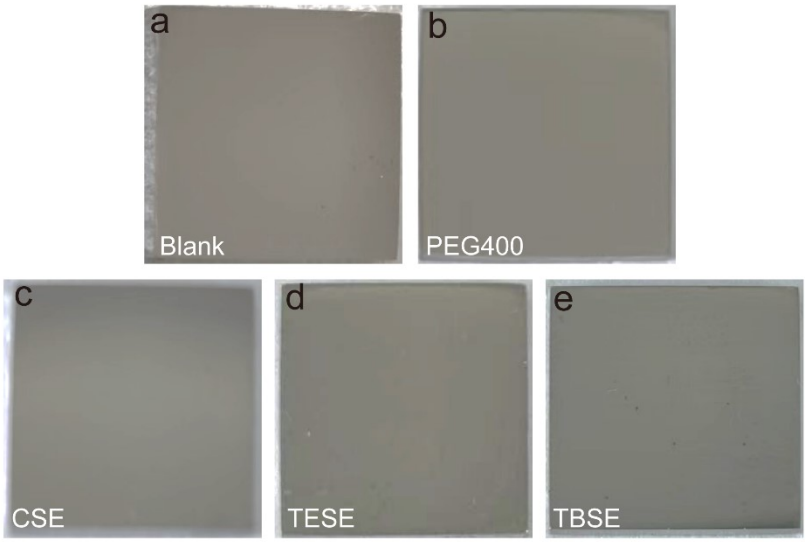

Fig. S4 Stainless steel images exposed to PEG400 oil and the as-synthesized TDESs. (a) Blank, (b) PEG400, (c) CSE, (d) TESE and (e) TBSE.

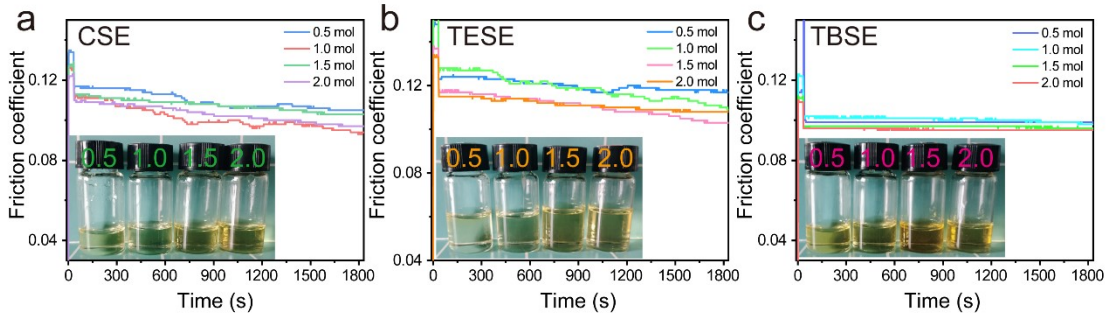

Fig. S5 Tribological properties about COF curves of the TDESs with various molar ratio under set condition. (a) CSE, (b) TESE, (c) TBSE. (SRV: 100 N, 25 ^{o}C, 25 Hz, 1 mm, 30 min, steel-steel).

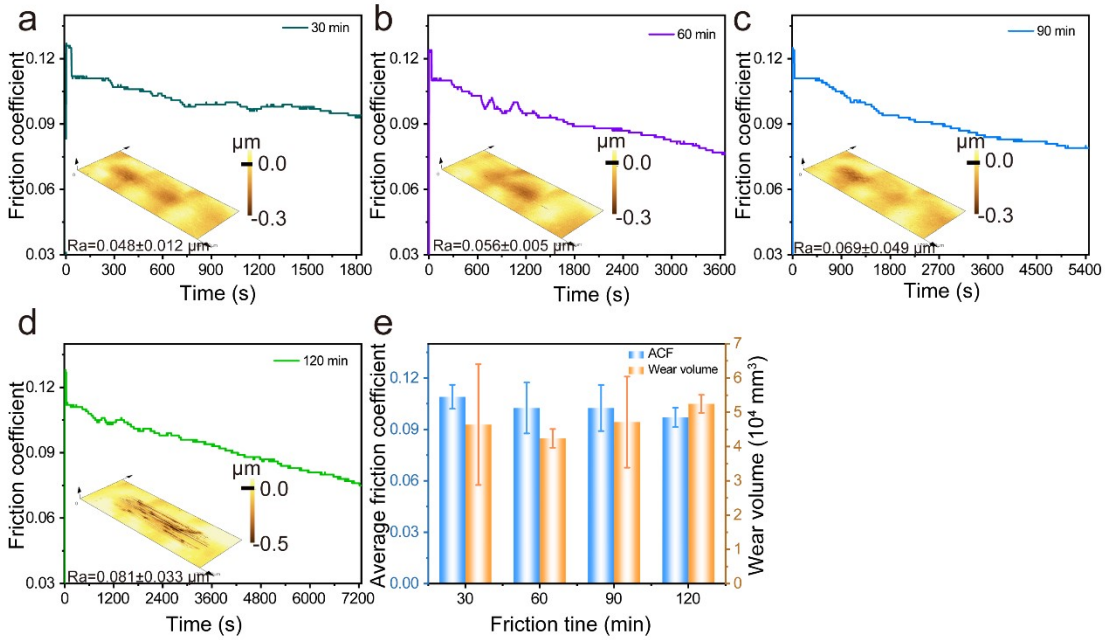

Fig. S6 Tribological properties of CSE TDES under the different test rime. (a) 30 min; (b) 60 min; (c) 90 min; (d) 120 min; (e) the corresponding ACF and average wear volume and (f) wear rates of wear disks.

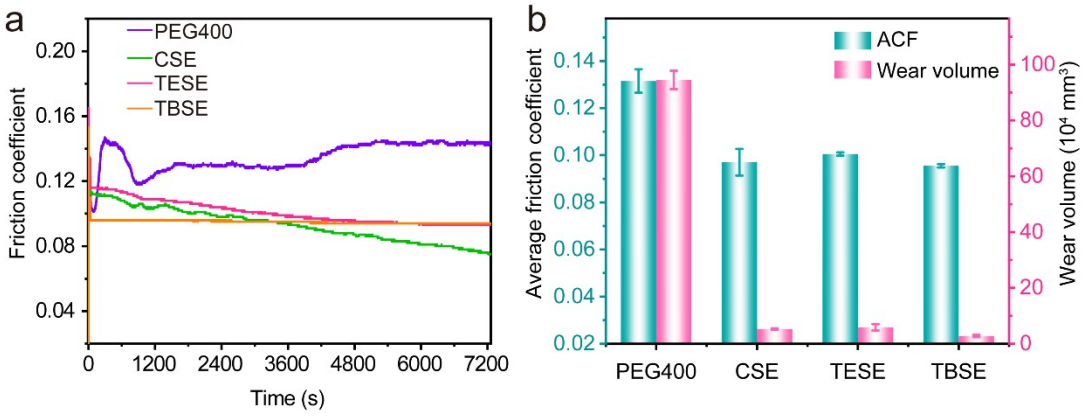

Fig. S7 Tribological properties of PEG400 oil and the synthesized TDESs. (a) friction curves, (b) ACF and wear volume for disks after a long-term friction period of 120 min. (SRV: 100 N, 25 °C, 25 Hz, 1 mm, steel-steel).

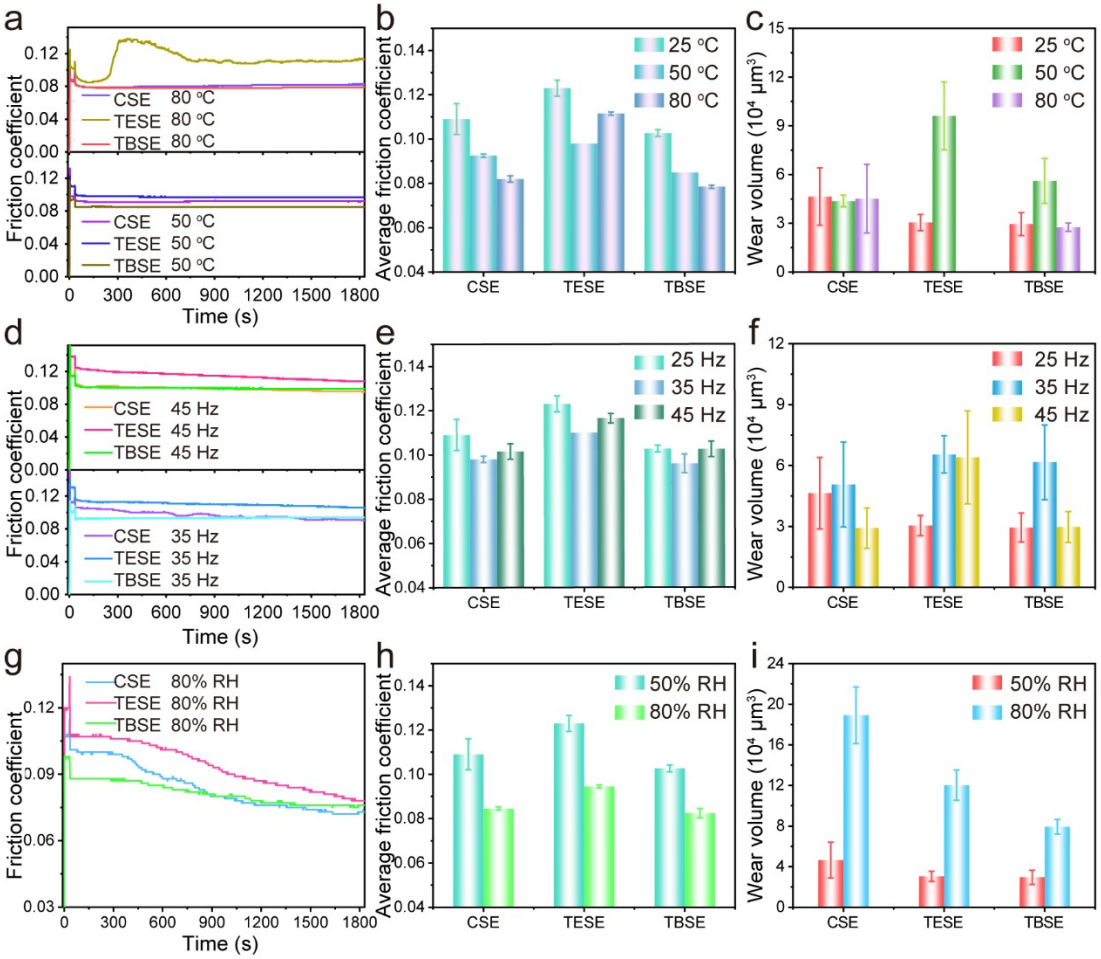

Fig. S8 Tribological performance of TDESs. Friction curves (COF), average friction coefficient (ACF) and wear volume of TDESs under different conditions, including (a-c) different temperatures (25, 50 and 80 °C), (d-f) different frequencies (25, 35 and 45 Hz) and (g-i) 50 and 80% RH.

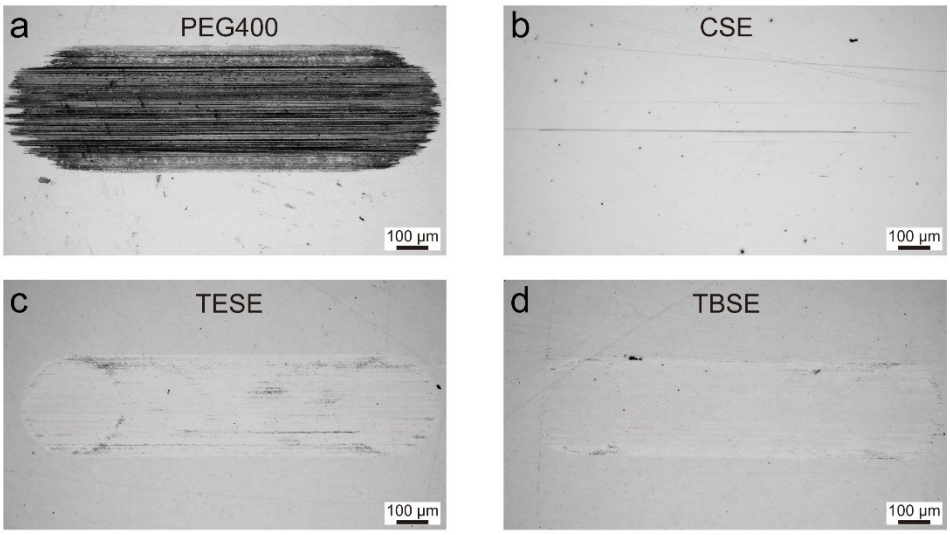

Fig. S9 Optical images of the worn scar on steel disk surfaces lubricated by (a) PEG400, (b) CSE, (c) TESE and (d) TBSE for the short-time friction process (30 min).

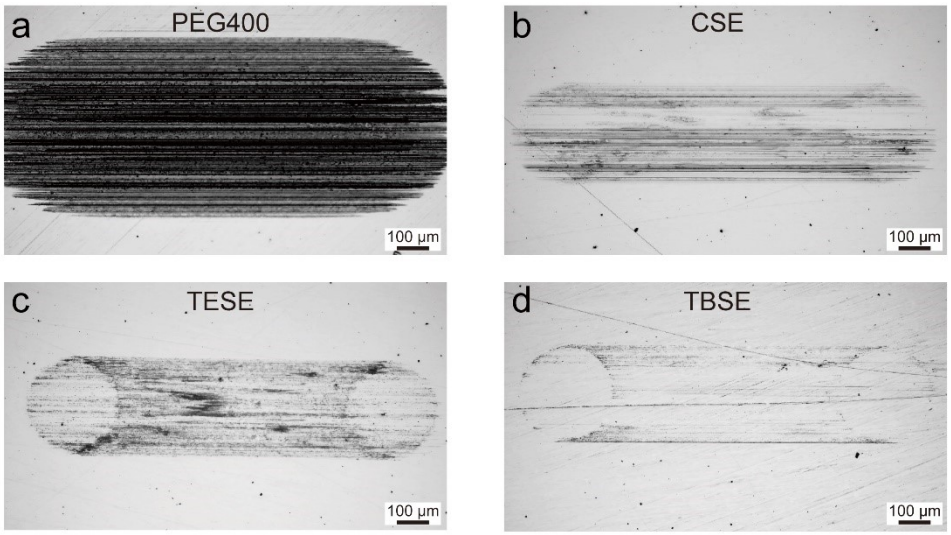

Fig. S10 Optical images of the worn scar on steel disk surfaces lubricated by (a) PEG400, (b) CSE, (c) TESE and (d) TBSE for the long-term friction process (120 min).

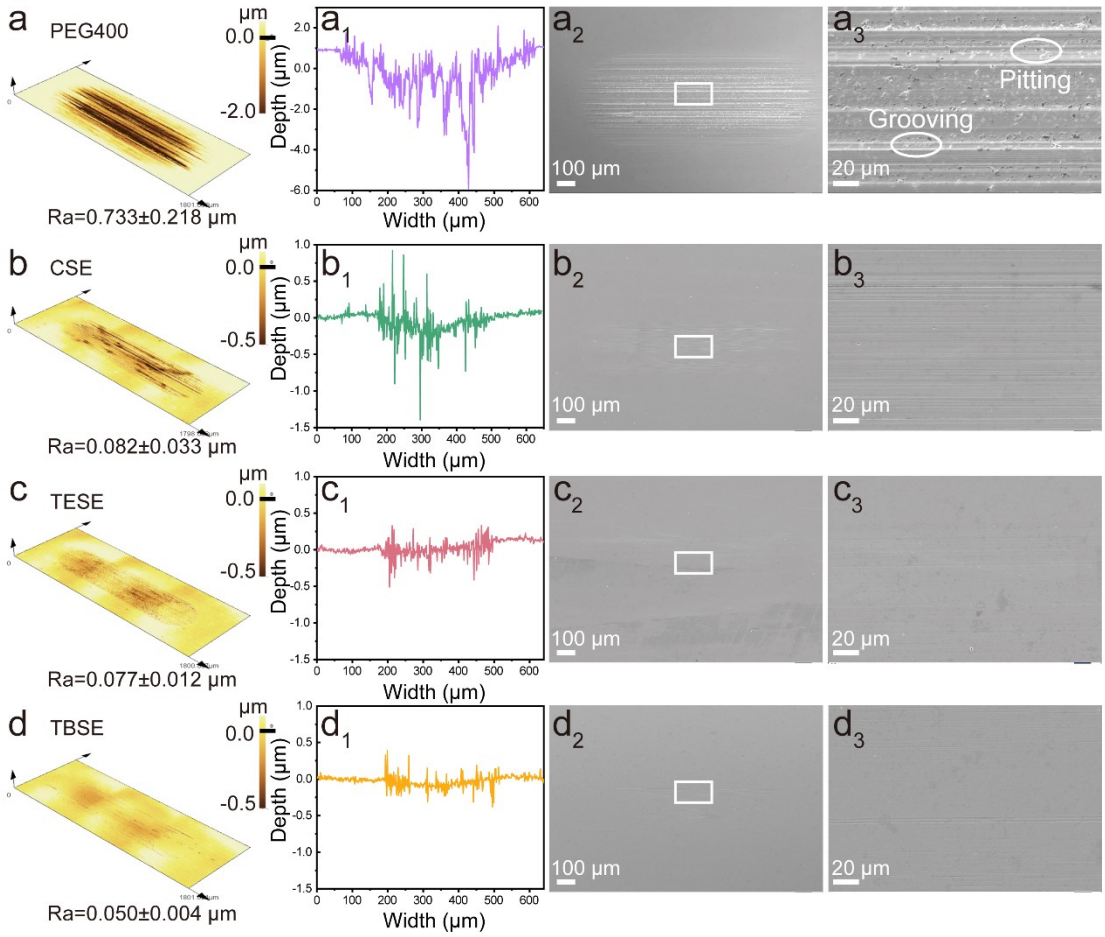

Fig. S11 Anti-wear performance. 3D microscopic morphologies, wear longitudinal profiles and SEM images of the worn scar on steel disk surfaces lubricated by PEG400 oil and the as-synthesized TDESs, (a, a_1-a_3) PEG400, (b, b_1-b_3) CSE, (c, c_1-c_3) TESE and (d, d_1-d_3) TBSE for the long-term friction process (120 min).

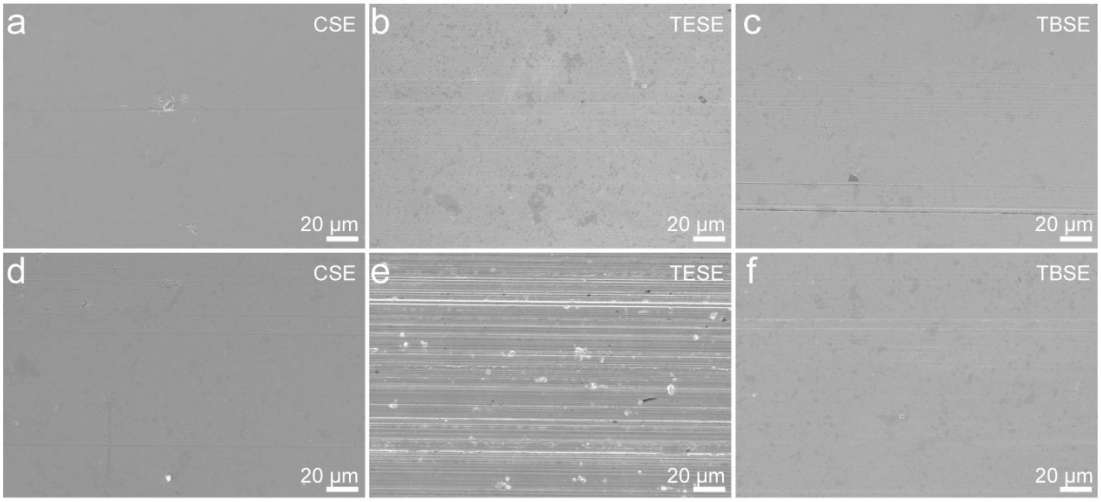

Fig. S12 Anti-wear performance. SEM images of wear tracks lubricated by (a,d) CSE, (b, e) TESE and (c, f) TBSE TDESs under various temperatures (a-c at 50 ^{o}C and d-f at 80 ^{o}C).

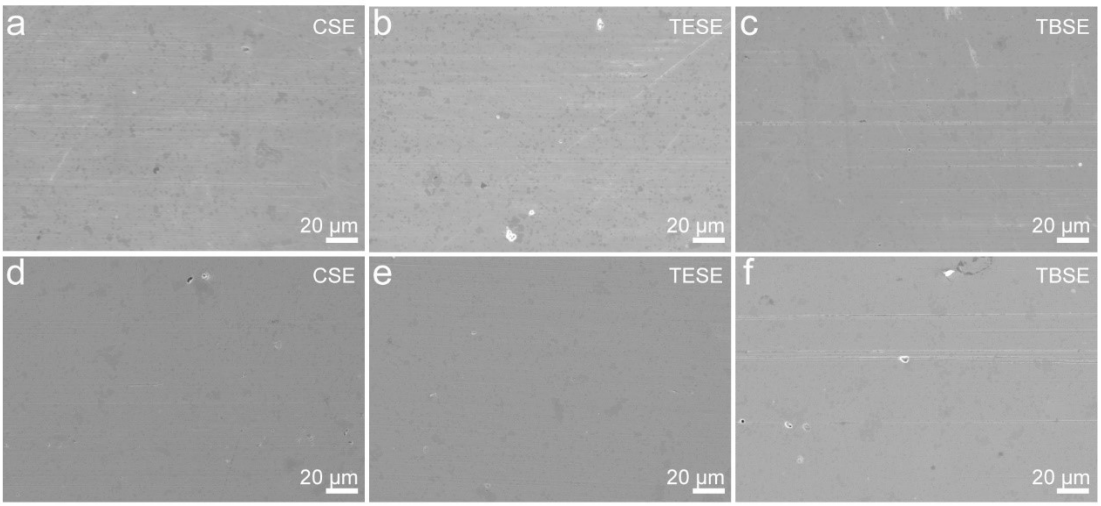

Fig. S13 Anti-wear performance. SEM images of wear tracks lubricated by (a, d) CSE, (b, e) TESE and (c, f) TBSE TDESs under various frequencies (a-c at 35 Hz and d-f at 45 Hz).

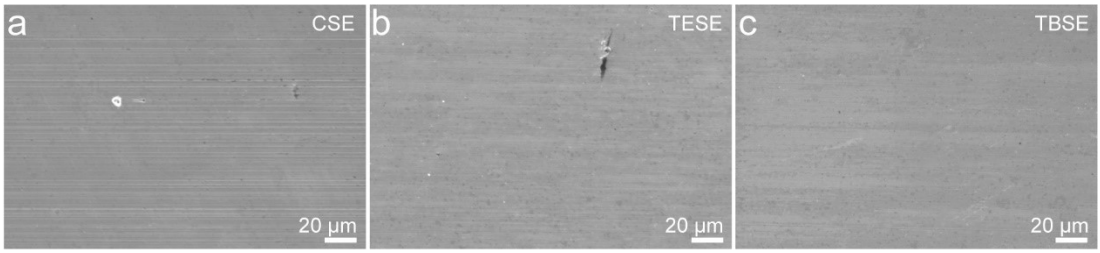

Fig. S14 Anti-wear performance. SEM images of wear tracks lubricated by (a) CSE, (b) TESE and (c) TBSE TDESs under high relative humidities (80% RH).

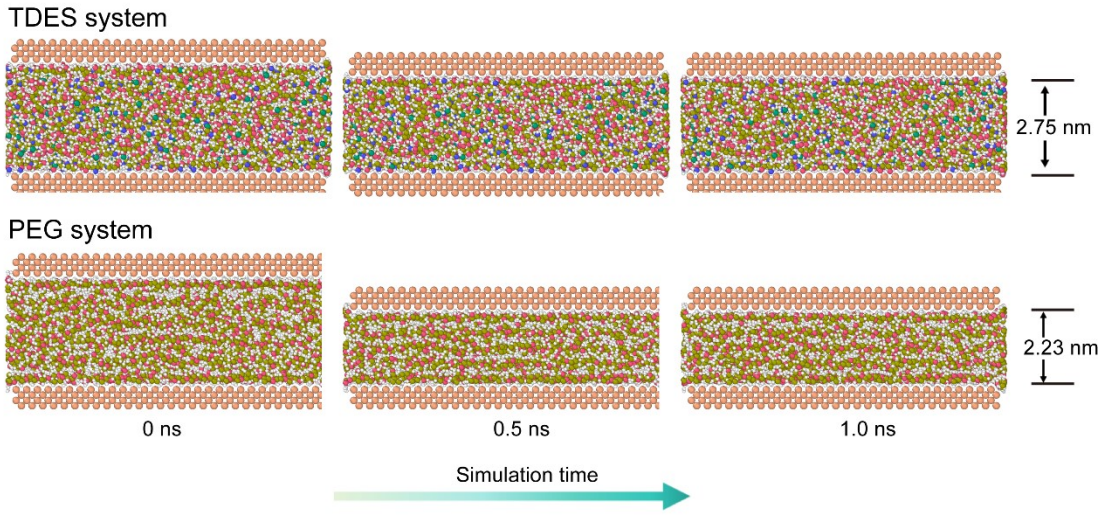

Fig. S15 The compressed simulation process and snapshots of two TDES and PEG systems.

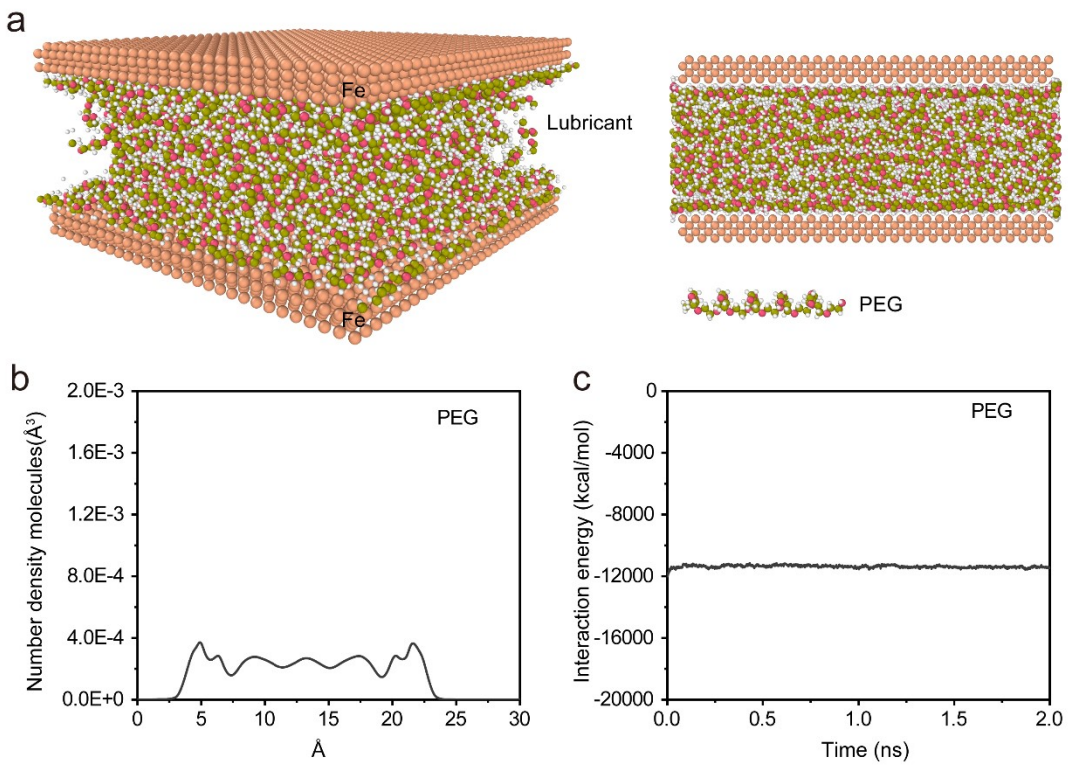

Fig. S16 Demonstration of the molecular dynamic simulation. (a) Detailed structure of designed model system including Fe, lubricant, and Fe; (b) Number density distribution of molecules in the slit after compression stabilization; (c) Interaction of molecules (PEG) toward the Fe substrate.

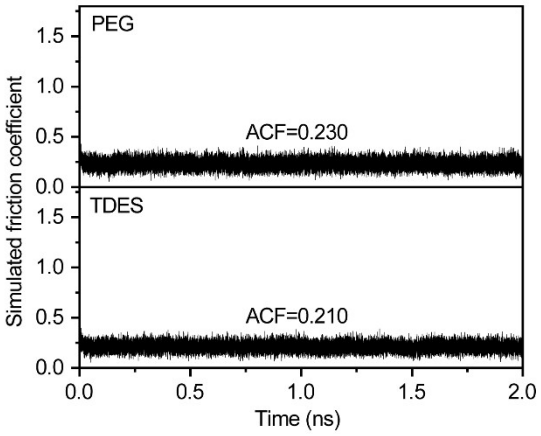

Fig. S17 The simulated friction coefficient curves of TDES and PEG.

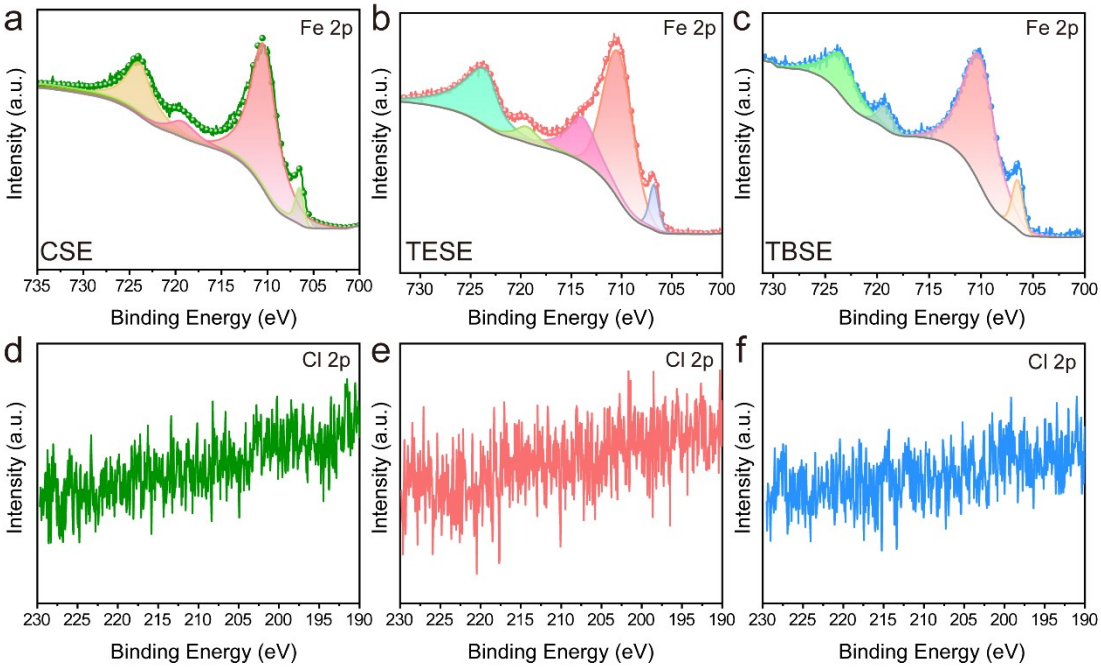

Fig. S18 XPS analyses of wear tracks. XPS spectra of the worn scar on steel disk surfaces lubricated by the as-synthesized TDESs, (a, d) CSE, (b, e) TESE and (c, f) TBSE. (a-c) Fe 2p and (d-f) Cl 2p. (SRV: 100 N, 25 ^{o}C, 25 Hz, 1 mm, 30 min, steel-steel).

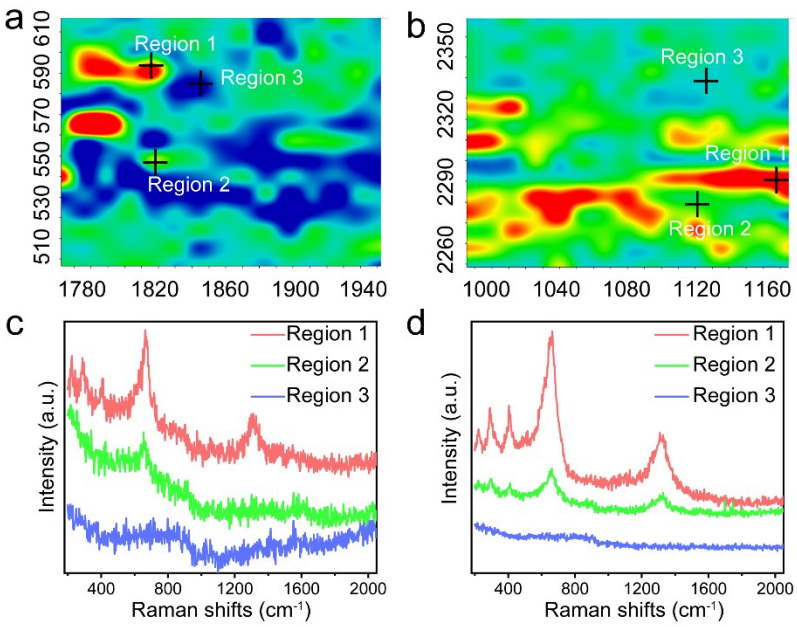

Fig. S19 Raman analyses of wear tracks. Raman mapping and the spectra corresponding to various color region of the worn scar on steel disk surfaces lubricated by (a, c) TESE and (b, d) TBSE tested for 30 min.

Table S1 Compositions, chemical Structures of raw materials, and abbreviations for as-synthesized TDESs.

HBD	T_m (°C)	HBA (QASs)	T_m (°C)	Abbreviation
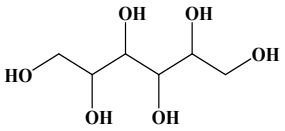	98-100	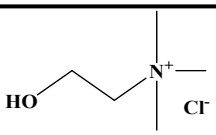	302-305	CSE
D-Sor		ChCl		
		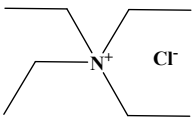	39	TESE
		TEAC		
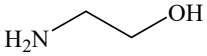	10-11	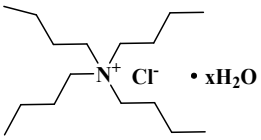	41-44	TBSE
EA		TBAC		

T_m: melting points (°C)

Table S2 Test parameters of the SRV tests.

NO.	Load (N)	Frequency (Hz)	Temperature (°C)	Amplitude (mm)	Test time (min)	Relative humidity (%)
1	100	25	25	1	30~120	50
2	100	25	25/50/80	1	30	50
3	100	25/35/45	25	1	30	50
4	100	25	25	1	30	50/80

Table S3 Studies on the near-wearless behavior.

NO.	Lubricants	Frictional pairs	Test instrument	Test conditions	Friction coefficient	Wear volume / rates	Test time	Lubricant mechanism	Ref.
i	-	Steel ball / a-C (a-C:H:O:F:Si)	Block on ring	2 N, 0.125 ms^{-1}, 4 mm, vacuum	~0.1	9.0×10^{-13} mm^3 N^{-1} mm^{-1}	$>2\times10^6$ cycles	Tribochemical reaction	[1]
ii	-	DLC film	-	5 N, 0.015 m/s, 4 mm, vacuum	0.001-0.005	10^{-10}-10^{-9} mm^3 /N m	2000-6000s	The hydrogen-terminated carbon surface	[2]
iii	LC-EG	Si_3N_4 / a-C	UMT-5	11 N, 2-810 rpm, 4 mm, 24 ºC	0.002	4.5×10^{-10} mm^3 /N m	1800s	Tribochemical reaction	[3]
iv	-	Steel ball / Si-DLC/PLC	Block on ring	20 N, 4 Hz, 4 mm, RT, N_2	0.003	4.06×10^{-9} mm^3 / N m	3000-100000 cycles	High-stress adaption and robustness of the antifriction features	[4]
v	-	Steel ball / Si-DLC/PLC	Block on ring	50 N, 4 Hz, 4 mm, 25 ºC	0.001	3.13×10^{-9} mm^3 /N m	3000 cycles	Construction of easy shear friction layer	[5]
vi	CF-4 diesel oil	Al_2O_3 ball-Cr-based coatings	SRV-IV	100 N, 20 Hz, 1 mm, RT	0.12-0.15	(4-9) $\times 10^5$ μm^3	30-150 min	The intrinsic characteristics of Cr-based coatings	[6]
vii	TDESs	Steel ball-disk	SRV-V	100 N, 25 Hz, 1 mm, RT	~0.1	10^{-10}-10^{-9} mm^3 /N m	30-120 min	The polar adsorption and tribochemical reaction	This work

Table S4 XPS peak fitting results for worn track lubricated by TDESs.

Region	CSE		TESE		TBSE		Ref.
	Binding energy (eV)	Assigned to	Binding energy (eV)	Assigned to	Binding energy (eV)	Assigned to	
C 1s	284.8	C-C	284.8	C-C	284.8	C-C	
	285.4	C-O / C-N	286.6	C-O / C-N	285.2	C-O / C-N	
		C=O		C=O		C=O	[7, 8]
	288.4	iron carbonate	288.5	iron carbonate	288.7	iron carbonate	
O 1s	529.6	iron oxide	529.7	iron oxide	529.4	iron oxide	
	531.1	Fe-O / C-O	531.6	Fe-O / C-O	531.3	Fe-O / C-O	[9, 10]
Fe 2p	706.5	Fe	706.8	Fe	706.5	Fe	
	710.4	FeO	710.3	FeO	710.0	FeO	
		Fe_2O_3,		Fe_2O_3,		Fe_2O_3,	[11, 12]
	723.9	Fe_3O_4 / FeOOH	723.5	Fe_3O_4 / FeOOH	723.3	Fe_3O_4 / FeOOH	
	719.1	satellite	719.4	satellite	719.2	satellite	[13]
			713.9	Fe_2O_3			[11, 12]
N 1s	399.8	C-N	399.8	C-N	399.5	C-N	
	402.6	C-N	402.1	C-N			[14, 15]

Calculation of oil film thickness and lubrication state:

To identify the lubricating state of the as-synthesized TDESs on steel surface, the minimum film thickness (h_{min}) between the contact interface of friction pairs is calculated according to the Hamrock-Dowson (H-D) theory of point contacts as follows equation:[16]

$$h_{min} = 3.63\frac{G^{0.49}U^{0.68}R}{W^{0.073}}\left(1 - e^{-0.68k}\right)$$

where $G = \alpha E$, $U = \eta\nu/ER$ and $W = F/ER^2$. In detail, η is the dynamic viscosity of the as-synthesized TDESs (as seen in Fig. 1f) and PEG400 oil (0.0949 Pa·s). ν (0.05 m/s) is the average sliding speed during the friction process. α (15×10^{-9} Pa^{-1}) is the viscosity-pressure coefficient of liquid lubricants. F is the applied normal load (100 N) and k (≈1) is the ellipticity of steel ball. R (~ 5 mm) is the radius of the steel ball. E is the equivalent elastic modulus of friction pairs and can be calculated by the follow equation:

$$\frac{2}{E} = \frac{1-\mu_1^2}{E_1} + \frac{1-\mu_2^2}{E_2}$$

where μ is the Poisson ratio of the material of the friction pairs. Based on the calculation results, the h_{min} of CSE, TESE, TBSE and PEG400 oil is 380.6, 193.5, 507.4 and 58.9 nm, respectively. Furthermore, the lubrication state of the as-synthesized TDESs can be evaluated by the thickness-roughness ratio (λ) by the follow equation:[17]

$$\lambda = \frac{h_{min}}{\sqrt{\sigma_1^2 + \sigma_2^2}}$$

where σ_1 and σ_2 are Ra of disk and ball of friction pairs, which was about 30 nm and 20 nm, respectively. Finally, the values of λ of CSE, TESE and TBSE can be calculated and are 10.55, 5.37 and 14.07 respectively, which are higher than 3. The results illustrate that the lubrication state of TDESs located in the region of full-film or elastohydrodynamic lubrication (hydrodynamic lubrication, HDL). However, the λ value of PEG400 oil is 1.63 (1~3), illustrating that the lubrication regime of PEG400 oil is the mixed lubrication.[18] Meanwhile, high calculated thickness of the lubricating film indicates that the as-synthesized TDESs could effectively restrain the direct contact of friction pairs, which beneficial to achieve the ultra-low wear performance on the steel surface.

References

1 L. Wang, R. Zhang, U. Jansson and N. Nedfors, *Sci. Rep.*, 2015, **5** 11119.

2 A. Erdemir, *Tribol. Int.*, 2004, **37**, 1005-1012.

3 S. Sun, S. Yi, J. Li, Z. Ding, W. Song and J. Luo, *ACS Appl. Mater. Interfaces*, 2023, **15**, 19705-19714.

4 W. Deng, Y. Wang, X. Chen, W. Qi, X. Li, C. Zhang, Q. Yu and J. Xu, *Appl. Surf. Sci.*, 2022, **595**, 153535.

5 W. Deng, Y. Wang, Q. Yu, X. Chen, P. Huang, X. Yu, W. Qi, X. Li, C. Zhang and J. Luo, *ACS Appl. Mater. Interfaces*, 2022, **14**, 51564-51578.

6 A. Liang, Y. Wang, F. Wang and L. Qiang, *Mater. Lett.*, 2022, **319** 132228.

7 F. Xu, H. Li, B. Tian, K. Cui, R. Dong, M. Fan, M. Cai, F. Zhou and W. Liu, *ACS Sustain. Chem. Eng.*, 2023, **11**, 8651-8666.

8 S. Liu, Q. Gao, K. Hou, Z. Li, J. Wang and S. Yang, *Chem. Eng. J.*, 2023, 142238.

9 N. S. McIntyre and D. G. Zetaruk, *Anal. Chem.*, 1977, **49**, 1521-1529.

10 E. Paparazzo, *J Electron. Spectrosc.*, 1987, **43**, 97-112.

11 Q. Ye, S. Liu, J. Zhang, F. Xu, F. Zhou and W. Liu, *ACS Sustain. Chem. Eng.*, 2019, **7**, 12527-12535.

12 Q. Gao, S. Liu, K. Hou, X. Miao, Z. Li and J. Wang, *Tribol. Int.*, 2023, **186**, 108652.

13 C. Zhou, Z. Li, S. Liu, L. Ma, T. Zhan and J. Wang, *Tribol. Lett.*, 2022, **70**.

14 S. Liu, Y. Jing, T. Zhang, J. Zhang, F. Xu, Q. Song, Q. Ye, S. Liu and W. Liu, *Chem. Eng. J.*, 2021, **412**.

15 R. Dong, L. Bao, Q. Yu, Y. Wu, Z. Ma, J. Zhang, M. Cai, F. Zhou and W. Liu, *ACS Appl. Mater. Interfaces*, 2020, **12**, 39910-39919.

16 X. Ge, T. Halmans, J. Li and J. Luo, *Friction*, 2019, **7**, 625-636.

17 T. Han, C. Zhang and J. Luo, *Langmuir*, 2018, **34**, 11281-11291.

18 T. Han, S. Yi, C. Zhang, J. Li, X. Chen, J. Luo and X. Banquy, *J. Colloid Interface Sci*, 2020, **579**, 479-488.